

RECENT DEVELOPMENT IN DOPPLER SONAR TECHNOLOGY

ROBERT PINKEL, MARK MERRIFIELD AND
JEROME SMITH

Marine Physical Laboratory
Scripps Institution of Oceanography
University of California, San Diego
9500 Gilman Drive
La Jolla, California 92093

INTRODUCTION

There has been significant recent progress in the development of Doppler sonar systems for marine research. Major advances include the development of side-scan Doppler systems for surface wave, ship wake and Langmuir cell research, the development of coded pulses for improved sonar precision, and the development of phased array Doppler sonar for 3-D (x, y, t) imaging of flow fields. Perhaps surprisingly, the Arctic has emerged as a prominent testing ground for many of these new technologies. The combination of a stable platform (the sea-ice) and extremely low natural signal levels enables accurate quantification of system performance. In the first section of this work we outline an approach to pulse coding which we have been exploring, with the objective of improving sonar precision. The second section reviews experience gained in the 1989 Coordinated Eastern Arctic Experiment, CEAREX and the 1992 Beaufort Sea Experiment, LEADEX. A brief discussion of a new phased array system we are developing for three dimensional observations concludes the work.

CODED PULSE DOPPLER SONAR

Performance bounds on simple Doppler systems can be estimated using methods derived for atmospheric acoustic and radar research. Theriault⁴ gives a simple approximate relation for the incoherent sounder, based on estimation of the Cramer-Rao bound:

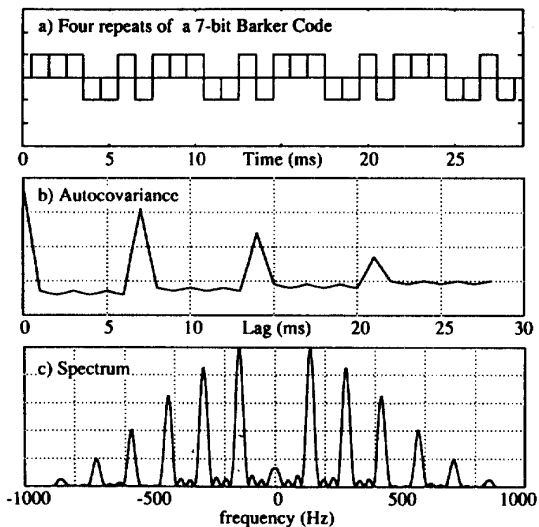


Fig. 1. (a) Schematic representation of a repeat-sequence code. The transmitted wave form consists of a 7-bit Barker code repeated four times. (b) The autocorrelation function of the repeat sequence code presented in (a). Values are small except at even multiples of the subcode length. (c) The frequency spectrum of four repeats of 7-bit Barker code. The spectrum of an uncoded sinusoidal pulse of the same duration would consist of a single peak of width equal to the width of any individual peak in the above spectrum.

$$\Delta V \Delta R = K c^2 f^{-1} P^{-1/2} \quad 1)$$

where ΔV is the rms velocity imprecision, ΔR is the effective range resolution $\approx cT/2$, where T is the duration of the transmitted pulse, c is the speed of sound, f is the acoustic frequency, and P is the number of independent incoherent averages used in forming the velocity estimate (eg, the number of transmissions). With f in Hz, the Cramer-Rao lower bound for K is $1/(8\pi)$.

Velocity precision increases with acoustic operating frequency. However, acoustic attenuation also increases with frequency. There is a tradeoff between the maximum range achievable with a given system and the expected range-velocity precision. Only by increasing the information content of the returning echo can one exceed the bounds mandated by (1).

For the 1989 Coordinated Eastern Arctic Experiment (CEAREX), a simple coding scheme was developed - repeat sequence coding. While the method is perhaps sub-optimal from a signal processing perspective, it is easy to implement and robust with respect to the scattering environment. Repeat-sequence codes are produced by taking a broad-band "subcode" and repeating it sequentially. The subcode is selected with the objective of having minimal self-correlation, except

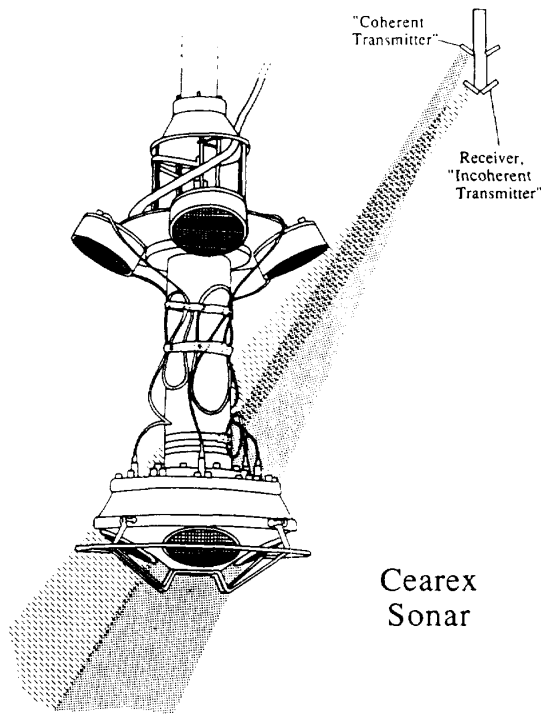


Fig. 2. The 161 kHz CEAREX sonar.

at zero lag. We consider here codes generated by reversing the sign of the carrier of the system at controlled intervals. The transmitted signal can be modeled as a sinusoid that is multiplied by either 1 or -1, depending on the dictates of the code. The seven-bit Barker code is shown in Fig. 1 as an example. For an ideal digitally synthesized subcode of bandwidth $1/\tau$ and duration $L\tau$, the time-bandwidth product is the number of "bits" in the subcode, L . If the subcode is repeated M times, the time-bandwidth product of the overall transmission is ML . If the subcode is properly chosen, the auto correlation of the overall transmission is nearly zero, except at $T_{lag} = nL\tau$, $n = 0$ to $M-1$ (Fig. 1b). The number of peaks in the code spectrum is roughly proportional to the number of bits, L , in the subcode (Fig. 1c).

Repeat sequence codes are contemporary analogs of the simple "pulse train" sequences developed in the early days of radar. A pulse train is a sequence of M sinusoidal pulses, each of length τ , transmitted at intervals of $L\tau$. The pulse train has an auto correlation which is exactly zero except at lags $NL\tau$, $N=1$ to $M-1$. The pulse train represents the ideal limit of the repeat sequence codes discussed here. However, the average power transmitted in a pulse train is low relative to the peak power. Repeat sequence codes approximate the pulse train ideal, but the average power transmitted is a factor of L greater. A longer useful range can be

achieved with the continuous code than with the pulse train.

The repeat sequence code also generalizes the pulse-pair approach investigated by Edwards⁵ and more recently by Brumley et. al.⁶. We consider the option of repeating the pulse or sequence more than just once. This enables the overall transmission length to be specified independent of the maximum unambiguous velocity, which is determined by the interpulse spacing, $L\tau$. This generalization is useful in adapting systems to different environmental conditions.

To estimate the Doppler shift of the echo, one simply calculates the auto covariance of the return at the single time lag $L\tau$. If the signal has been previously complex demodulated, the phase of the complex auto covariance is proportional to the Doppler shift⁷. The statistical stability of the covariance estimate can be improved by averaging over successive returns, at fixed range, and by averaging in range from a single transmission.

It is in the process of range averaging that the coding gives rise to substantial improvement over conventional transmissions. In averaging over L consecutive samples, the pulse train yields L independent estimates, whereas estimates from an uncoded transmission are highly correlated. Following the averaging process, both in range and in time (over successive returns) the performance of the coded pulse is given by:

$$\Delta V \Delta R = \frac{1}{4\pi} \left(\frac{3c^3 V_{\max}}{2Pf\Delta f} \right)^{1/2} \quad 2)$$

Here it is assumed that range resolution is given by $\Delta R = (n-1)L\tau c/2$ and that range averaging is performed over the corresponding interval ΔR . The maximum velocity one can resolve, without aliasing is $V_{\max} = c / (4f\tau L)$.

Equation 2 is useful in addressing both operational and system design issues. It illustrates the capability to customize repeat sequence codes for specific velocity variability situations, V_{\max} , in addition to standard range-velocity precision constraints. This allows greater flexibility in operation than single pulse-pair codes, which represent the low V_{\max} limit of the repeat sequence family.

In designing or modifying sonar systems, equation 2 indicates that net performance will vary as $(f\Delta f)^{-1/2}$. One can improve performance of an existing fixed-frequency system by increasing the bandwidth. Conversely, in considering new systems, one can double the bandwidth of a benchmark design and halve the carrier frequency, while maintaining performance. The lower-frequency sonar will have significantly greater overall range.

THE CEAREX 161 KHZ SONAR

In the summer of 1988, work was initiated on a sonar system which incorporated the coded pulse technology. The sonar was designed to operate at 161 kHz, at a peak power of 1.1 KW, shared between four down-looking beams. The sonar was planned to operate in both pulse-to-pulse-coherent and in incoherent (coded pulse) modes (Fig. 2). The two operating modes were alternated in an interlaced fashion.

Coherent mode transmissions emanate from a set of four "upper" transducers. These were canted at a slight angle relative to the receivers, the "lower" transducers, which were directed 30° off vertical. The crossed beam geometry focused on the 40 m region nearest the sonar, de-emphasizing returns from greater ranges. The coherent transmission sequence consisted of a series of eight 1.33 ms pulses at intervals of 50 ms, followed by eight more at 40 ms spacing. The dual pulse repetition frequency was employed to assist in resolving the velocity alias problem.

Following the coherent pulse sequence, a single 8 ms coded pulse was transmitted from the lower transducer. The code consisted of 5 repeats of a 7 bit Barker code. The duration of each bit was .333 ms. This "long range" transmission was followed for .6 s, to a range of 450 m (a depth of 390 m) and processed in a pulse-to-pulse incoherent fashion, as described above.

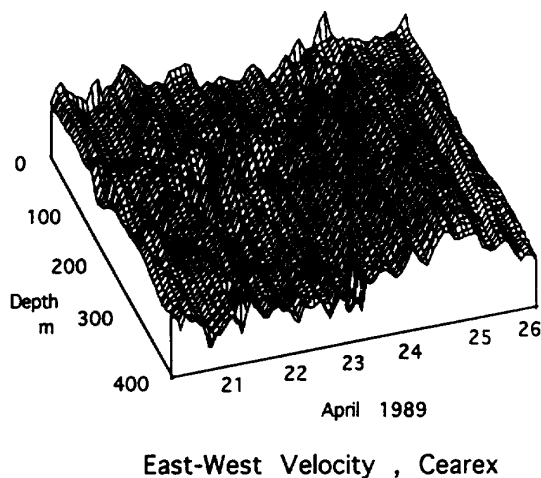


Fig. 3. East-West velocity as a function of depth for the final six days of the experiment. The eddy drifts under the ice camp on 23-26 April, with peak speeds of 20 cm s^{-1} . Tidal motion of long vertical wavelength is apparent throughout the record.

OBSERVATIONS

The 161 kHz sonar was deployed in April 1989, at 83° N , 13° E at the CEAREX Oceanography Ice Camp. The camp was initially located in 3.5 km deep water, north of Fram Strait. It drifted first to the south-east, up the lower flank of the Yermak Plateau and then to the south-west, following the 2 km depth contour of the Plateau.

The sonar system was housed in a 8' by 16' tent. The transducer assembly was suspended from a rigid pipe string, with the coherent transmit transducers approximately 1 m below the base of the 2 m thick ice. The system operated nearly continuously from 4 to 26 April. Data were processed, displayed and recorded on a Macintosh IIx computer: 40 megabyte magnetic disks were used to record the data. Brief data gaps occurred when recording disks were changed and when camp power was interrupted to service the electrical generators.

In contrast with central Arctic observations, highly energetic motions were observed as the ice camp drifted along the flank of the Yermak plateau. Both semi-diurnal and diurnal tidal signals were strong. During the period of spring tides (13-18 April), the waves were sufficiently energetic as to go unstable, producing high frequency non-linear wave trains of significant amplitude⁸.

Of particular interest was a small anti-cyclonic eddy that drifted directly under the ice-camp, just prior to the termination of the experiment (Fig. 3). The eddy was

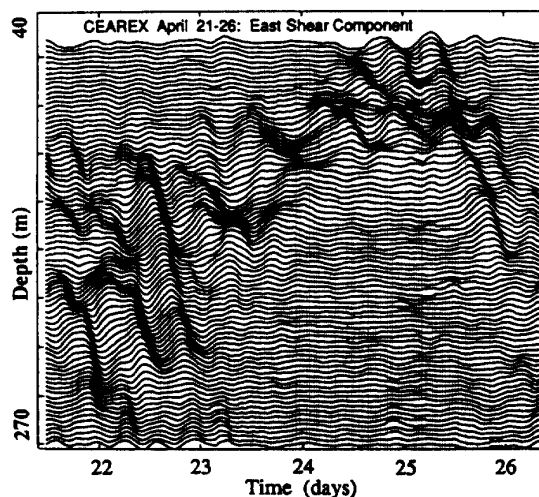


Fig. 4. East-West shear as a function of depth. Strong near inertial waves precede the arrival of the eddy and are seen above the dome of the eddy core. A near absence of shear is seen in the eddy interior.

advected in a diurnal tidal flow of significant energy, yet it dominated the overall current field, with current speeds reaching 20 cm s^{-1} . The eddy is estimated to have a radius of approximately 10 km and a rotation period of order 40 hrs. It is conjectured that the eddy was generated along the eastern edge of Fram Strait, where the northward flowing Atlantic water passes Svalbard.

Several aspects of the eddy are particularly interesting. The eddy appears sufficiently "young" that it has yet to reach equilibrium form. It is evidently radiating near inertial waves (Fig. 4) which precede the arrival of the eddy itself by several days. These have vertical wavelengths of order 100 m with downward propagating phases. The waves are radiating sufficient energy to drain the eddy of kinetic energy in several years. It is likely that the radiative process will diminish as the eddy assumes its equilibrium form and moves into the interior of the Arctic Ocean.

Evidently, the ambient internal waves are refracted or otherwise prevented from propagating into the eddy interior. This is seen by the near absence of shear in the interior of the eddy (Fig. 4). Hydrographic measurements (J. Morison, personal communication) confirm the relative isolation of the eddy core in terms of mixing. The water in the core is more representative of Atlantic inflow water than the local water of the basin. Acoustic scattering properties are slightly different in the core, suggesting that a different biological community is present. In particular, isolated "hard targets" are occasionally encountered in the eddy core, in contrast to the surrounding water. This suggests that a population of swimmers has either been advected in with the eddy or attracted to the eddy core by the plankton population.

LEADEX 1992

The LEADEX experiment was planned for the Beaufort Sea, with the objective of studying the oceanography and meteorology of winter leads. Two new instruments were designed for this effort. The first was a conventional four-beam downlooking sonar, representing an evolutionary advance over the CEAREX instrument. This transmitted a 5 kHz bandwidth code, measuring to depths in excess of 300 m with 2 m depth resolution. A second instrument produced a planar fan of 28 beams, and was designed for deployment at the edge of an open lead (Fig. 5). This used a 16 element phased array to form the beams.

We discuss briefly the result from the conventional downlooking sonar. This 155 kHz device transmitted 2 repeats of a 13 bit code, .2 ms per bit. Of particular interest, the sonar precision in LEADEX fell short of the theoretical limits outlined above. The deviation was ascribed to the unusual nature of the scattering field observed in the upper Beaufort Sea, following the dark,

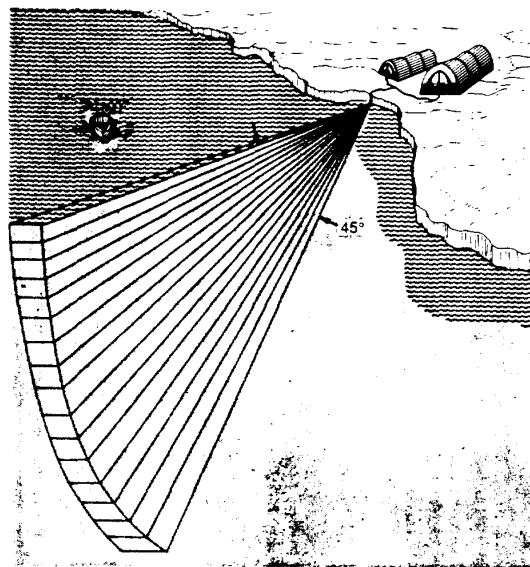


Fig. 5 Schematic diagram of the 195 kHz coded pulse sector-scan sonar deployed in the 1992 LEADEX experiment.

ice covered winter. Relative to more typical open-ocean environment the scattering was extremely non-homogeneous. Strong isolated "hard-hits" were the norm, with only occasional periods of homogeneous return (Fig. 6). The gain from the repeat sequence coding is realized through range averaging. When the scatterers are not distributed homogeneously, the benefit from this averaging is reduced. The contribution from the strongest scattering region dominates each average.

LEADEX represented the initial deployment of the Sector Scan Doppler sonar. This device transmits a 195 kHz coded pulse in a 45° planar sector. The signal is received by a 16 element phased array. Data are digitized at a rate of .3 Mbyte/s and are transmitted up optical fiber to the surface. Information is processed using a Macintosh Quadra computer with a National Instruments digital signal processing card. Sector-scan maps of scattering intensity and the radial component of velocity are produced in real time. In addition, "time-lapse movies" of the fields are accumulated. They can be replayed after each data update, typically 1-2 min.

The scientific objective of this open-lead experiment was to detect convective cells or other lead-related flows. The technical challenge was to observe flows in the center of a lead using instruments mounted at the lead edge. The sector-scan design was a response to this challenge. While convective activity was apparently not present at the lead visited (LEADEX "lead 3" 6-9 April 1992), a detailed set of vertical profiles of horizontal velocity was collected from the

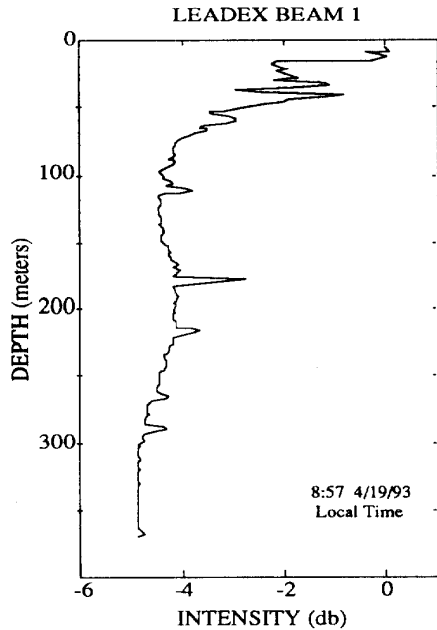


Fig. 6. Intensity of acoustic backscatter from the 155 kHz Doppler sonar deployed at the LEADDEX base camp.

central section (50-250 m range average) of the lead (Fig. 7). These showed weakly sheared flow in the mixed layer (0-30 m) with stronger shears in the waters below. Heat fluxes into the lead during this time were relatively weak. The absence of obvious convective activity is thus understandable.

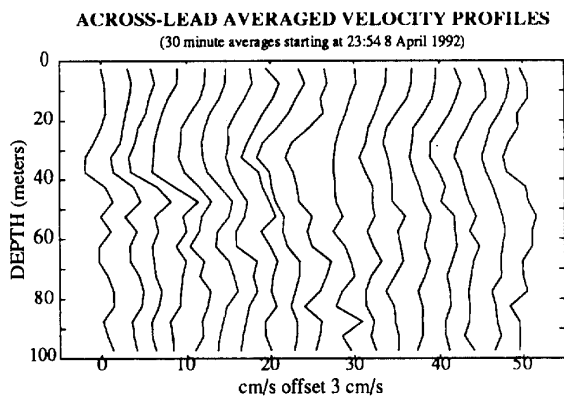


Fig. 7. A 9 hour observation of the cross-lead component of horizontal velocity.

Subsequent to LEADDEX, the downlooking 161 kHz system was converted to a shipboard configuration mounted on the R.V. John Vickers and operated throughout the Western Pacific ocean. The sector-scan system was also deployed from the Vickers during

October-December 1992, in the Western Equatorial Pacific. These measurements, obtained in conjunction with the TOGA COARE experiment, provided a cross sectional view of the upper edge of the equatorial undercurrent and the deeper reaches of the mixed layer. Analysis of these data are in progress.

SUMMARY

Arctic environmental science has encouraged development of a new generation of acoustic devices. In turn, the Arctic environment has provided a nearly ideal laboratory for the testing of new instruments and concepts. Given the scientific benefits achieved to-date, further cycles of research and development are anticipated.

ACKNOWLEDGMENTS

The authors would like to thank E. Slater, L. Green, M. Goldin, and C. Neeley for assistance in the design and creation of these instruments. This work was sponsored by the Office of Naval Research.

REFERENCES

- [1]. LEVINE, M.D., C.A.PAULSON, and J.H.MORISON. (1985). *Internal waves in the Arctic Ocean: comparison with lower-latitude observations*. J. Phys. Oceanogr., Vol. 15, 800-809.
- [2]. PLUEDDEMANN, A.J. (1992). *Internal wave observations from the Arctic Environmental Drifting Buoy*. Submitted to J. Geophys. Res.
- [3]. PADMAN, L. and T.M.DILLON. (1989). *Thermal microstructure and internal waves in the Canada Basin diffusive staircase*. Deep Sea Res., 36, 531-542.
- [4]. THERIAULT, K.B. (1986). *Incoherent multibeam Doppler current profiler performance. Part I: estimate variance*. J. Ocean Eng., Vol. OE-11(1), 7-15.
- [5]. EDWARDS, J.A. (1979). *Remote measurement of water currents using correlation sonar*. Presented at 98th meeting of the Acoustical Society of America, Salt Lake City, Utah.
- [6]. BRUMLEY, B., R.CABRERA, K.DEINES, and E.TERRAY. (1990). *Performance of a broadband acoustic Doppler current profiler*. Proc. of the IEEE Fourth Working Conference on Current Measurement. Institute of Electrical and Electronics Engineers, New York City, 283-289.
- [7]. PINKEL, R. (1981). *On the use of Doppler sonar for internal wave measurements*. Deep-Sea Res., Vol. 28A, 269-289.
- [8]. PADMAN, L.A., J.PLUEDDEMANN, R.D.MUENCH and R.PINKEL. (1992). *Diurnal tides near the Yermak Plateau*. Submitted to J. Geophys. Res.